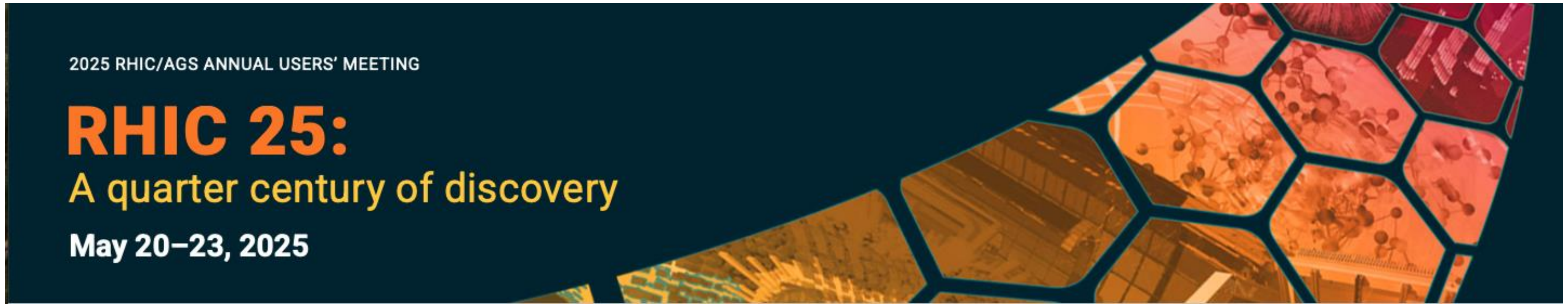


Brookhaven National Laboratory

U.S. DEPARTMENT OF ENERGY

# Recent results from fixed target beam energy scan data

Lijuan Ruan (BNL)

May 20, 2025

@BrookhavenLab

# The phases of QCD matter

Lattice QCD: crossover chiral transition at $\mu_B$ **< 3 T**

At top RHIC and LHC energies, measurements consistent with a smooth crossover chiral transition

Change T and $\mu_B$ by varying the collision energy:

- Search for the critical point
- Search for the first-order phase transition
- Search for the threshold of QGP formation

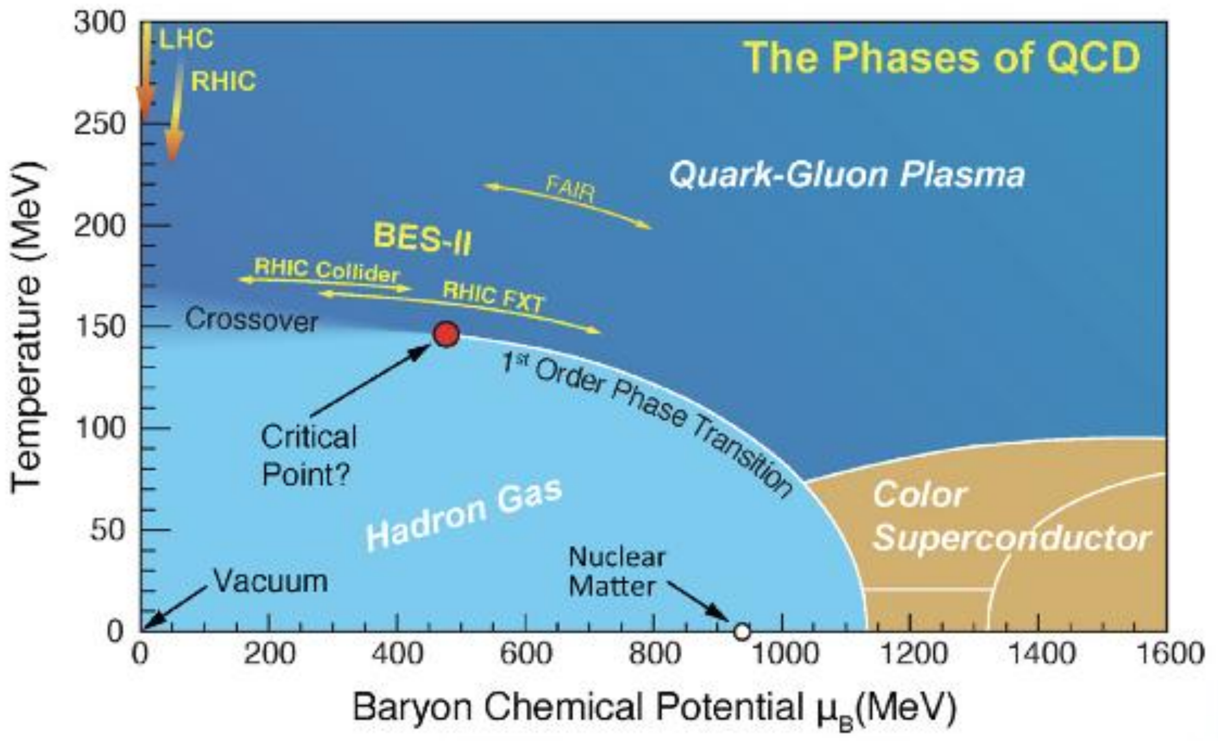

# STAR beam energy scan phase I campaign

In 2006, stated in the Beam Use Request:
definite search for the existence and location of the QCD Critical Point for Run 2009

RHIC Beam Energy Scan Phase I in 2010 and 2011

| Energy (GeV) | 7.7 | 11.5 | 19.6 | 27 | 39 | 62.4 | 200 |
|---|---|---|---|---|---|---|---|
| Statistics (Million) | ~3 | ~6.6 | ~15 | ~30 | ~87 | ~47 | ~242 |
| Year | 2010 | 2010 | 2011 | 2011 | 2010 | 2010 | 2010 |

Time of flight detector upgrade just completed before Run 2010

**RHIC Multi-Year Beam Use Request**
**For Run7 – Run 9**

**The STAR Collaboration**

*August 24, 2006*

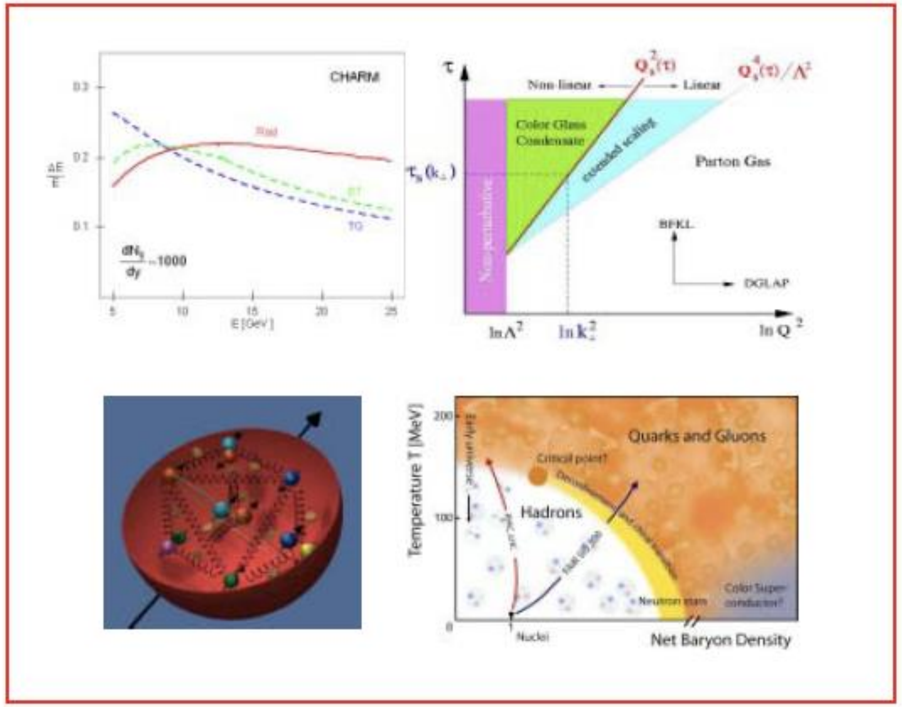

# STAR beam energy scan phase II campaign

## STAR Collaboration Decadal Plan
## December 2010



1

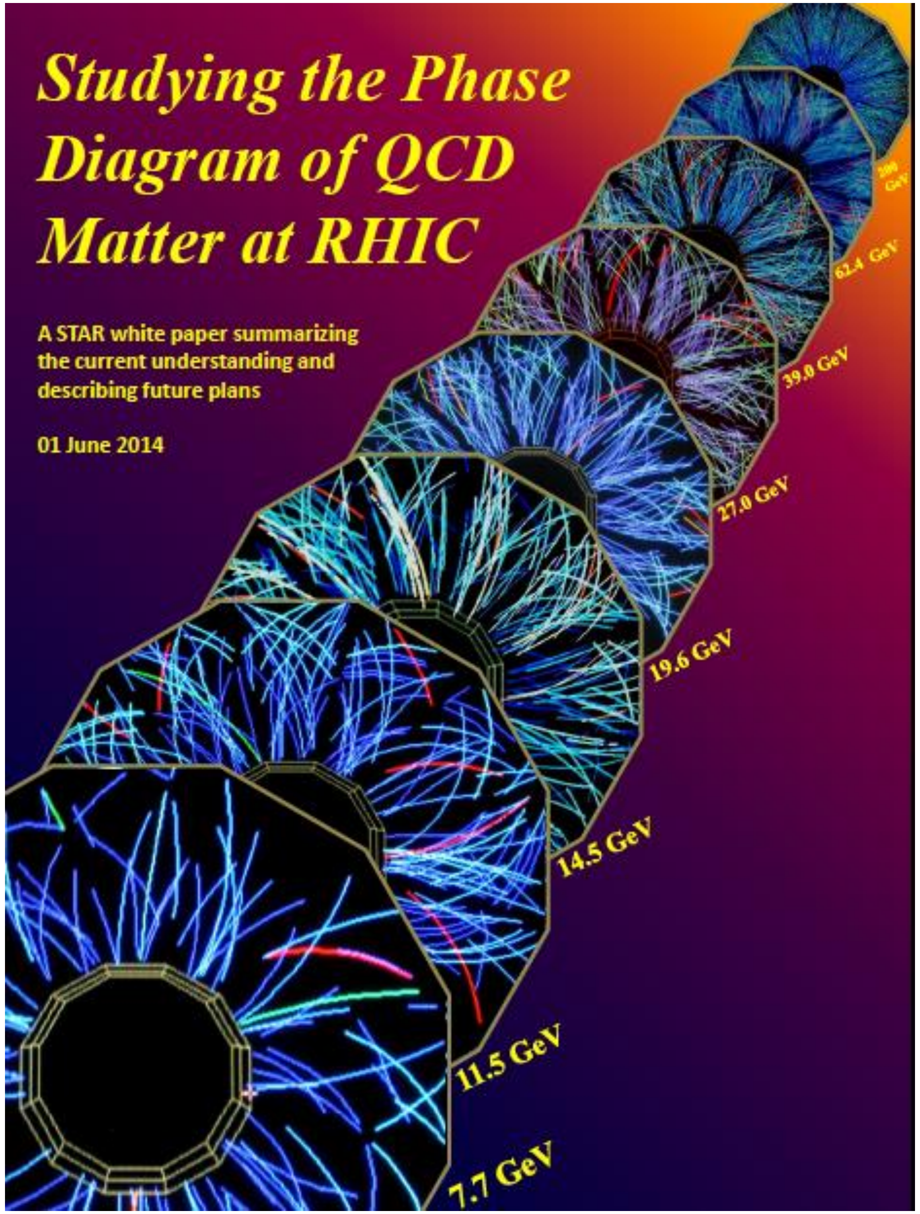


https://drupal.star.bnl.gov/STAR/starnotes/public/sn0598

# STAR as a fixed-target experiment

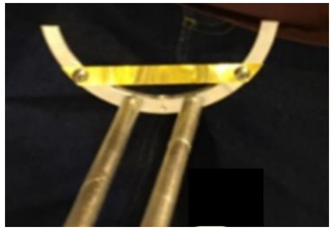

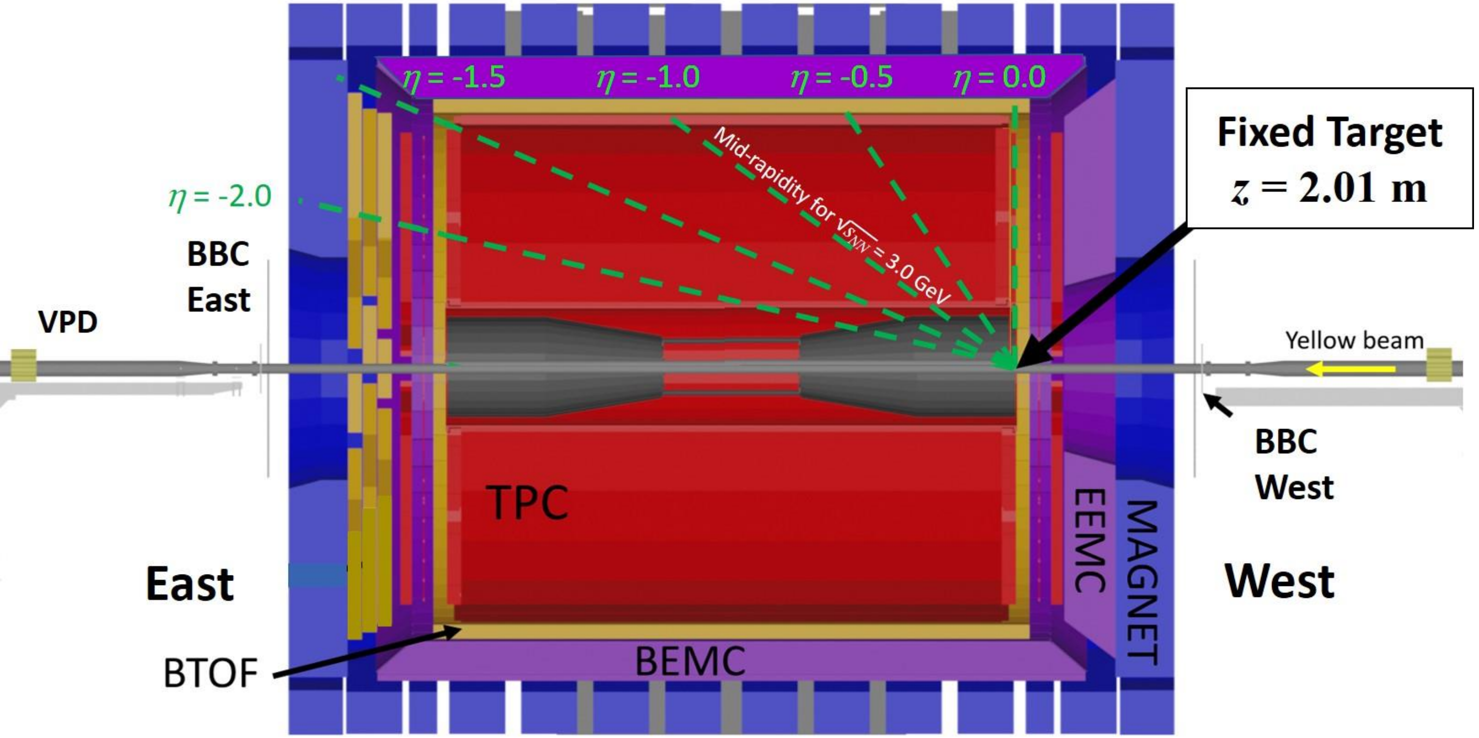


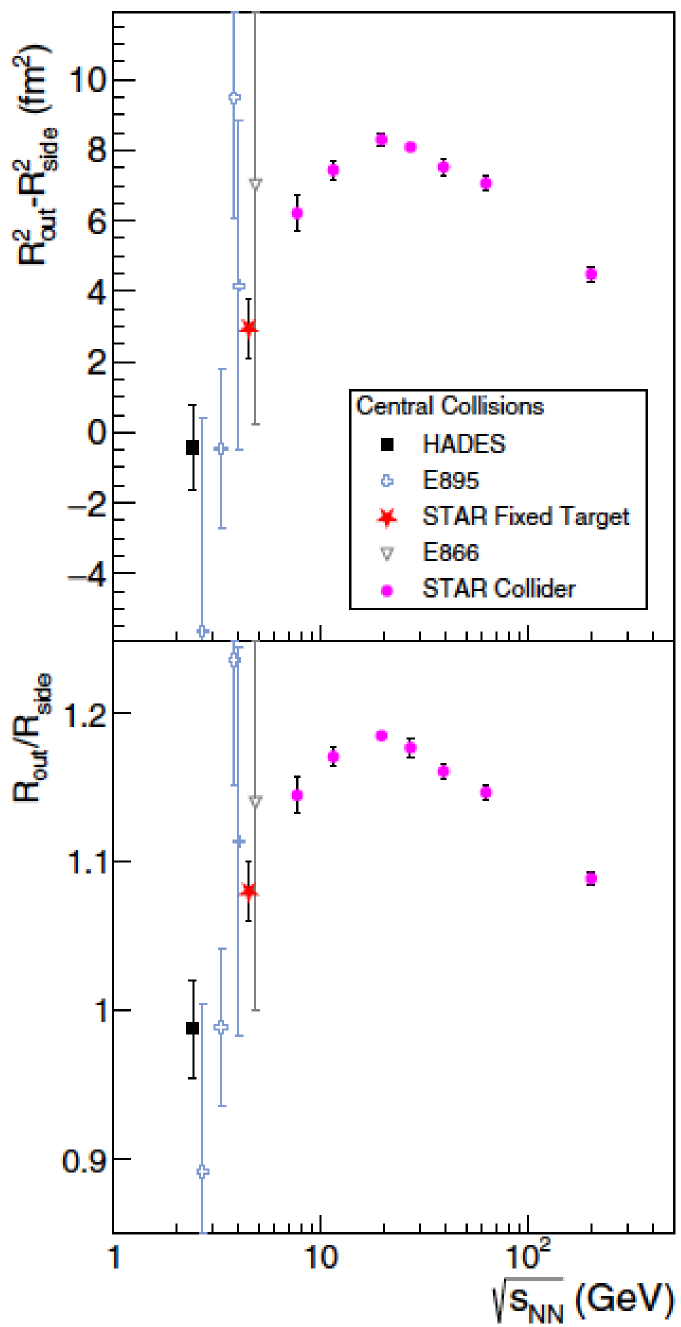


A gold target was installed inside the beam pipe in December 2013 for a feasibility test

– collected data during 14.5 GeV Run in 2014

A thinner gold target was installed for FXT program 2018-2021

# How to infer the QCD critical point

Divergence of the correlation length, dynamics slow down, Large density fluctuations

Critical opalescence, magnetic susceptibility

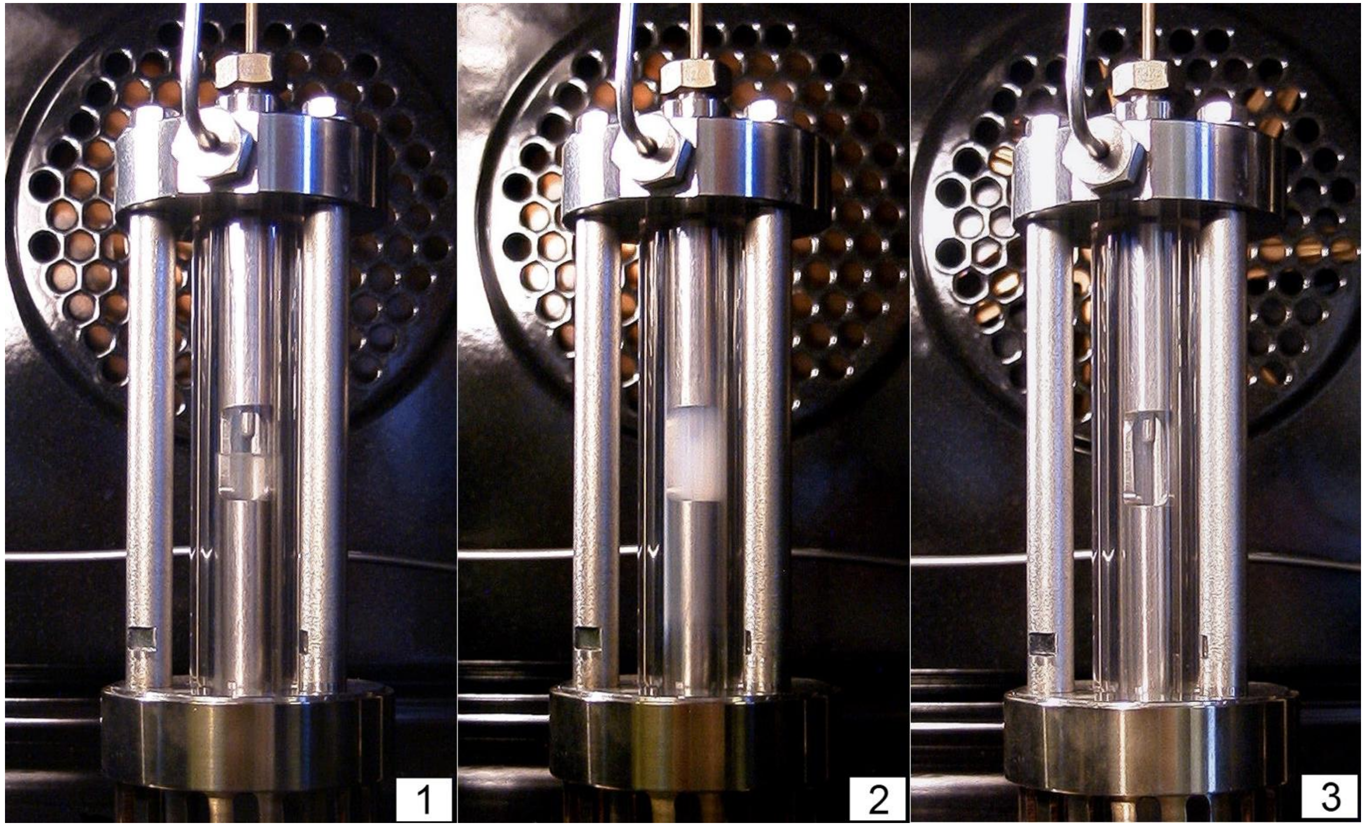

# How to infer the QCD critical point

Correlation length related to various moments of the distributions of conserved quantities such as net-baryon, net-charge, and net-strangeness.

$$<(\delta N)^2> \approx \xi^2, <(\delta N)^3> \approx \xi^{4.5}, <(\delta N)^4> - 3<(\delta N)^2>^2 \approx \xi^7$$

**Mean:** $M = <N>$

**St. Deviation:** $\sigma = \sqrt{<(N - <N>)^2>}$

**Skewness:** $S = \frac{<(N - <N>)^3>}{\sigma^3}$

**Kurtosis**: $\kappa = \frac{<(N - <N>)^4>}{\sigma^4} - 3$

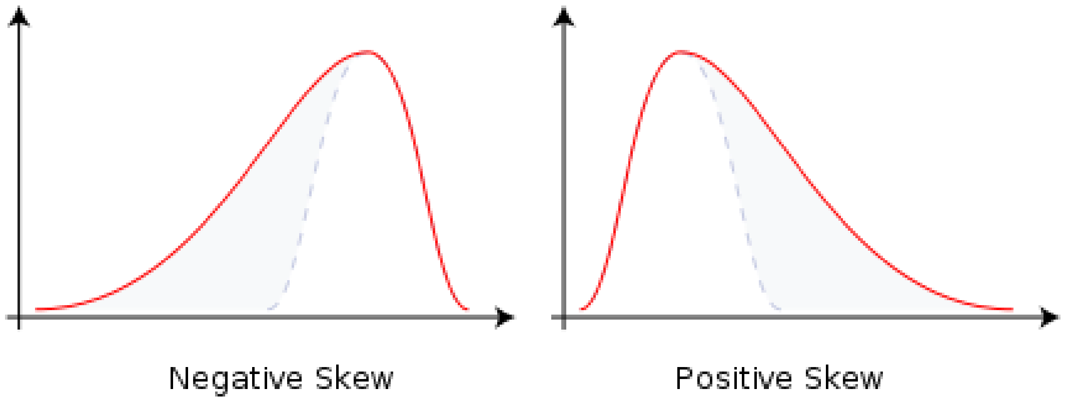


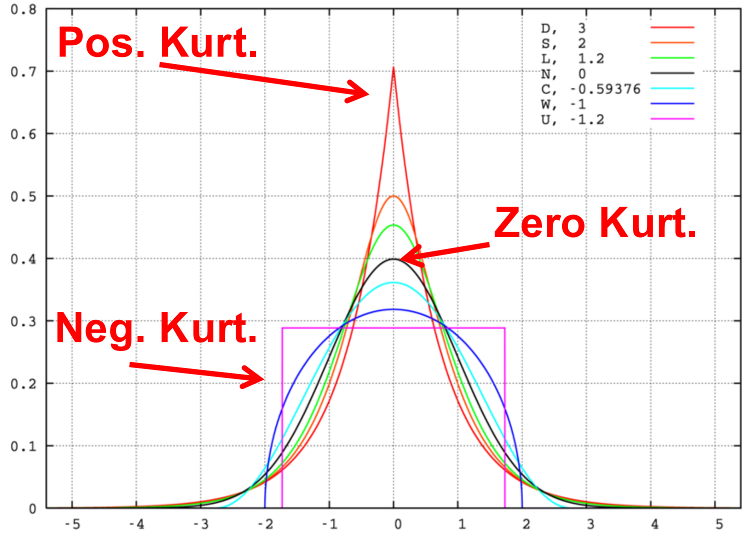


Measure non-Gaussian fluctuation of conserved quantities

# Connection to Lattice QCD

Lattice calculations show that moments of the conserved charge (net-baryon, net-charge, net-strangeness) distributions are related to the susceptibilities

**Pressure:**

$$\frac{p}{T^4} = \frac{1}{VT^3} \ln Z(V, T, \mu_B, \mu_Q, \mu_S)$$

**Susceptibility:**

$$\chi_q^{(n)} = \frac{1}{T^4} \frac{\partial^n}{\partial(\mu_q/T)^n} P\left(\frac{T}{T_C}, \frac{\mu_q}{T}\right)\Big|_{T/T_c},$$

$q = B, Q, S$ **(Conserved Quantum Number)**

$$\chi_q^{(1)} = \frac{1}{VT^3}\langle \delta N_q \rangle, \chi_q^{(2)} = \frac{1}{VT^3}\langle (\delta N_q)^2 \rangle$$

$$\chi_q^{(3)} = \frac{1}{VT^3}\langle (\delta N_q)^3 \rangle$$

$$\chi_q^{(4)} = \frac{1}{VT^3}\left( \langle (\delta N_q)^4 \rangle - 3\langle (\delta N_q)^2 \rangle^2 \right)$$

A. Bazavov et al *.arXiv::1208.1220. 1207.0784.*
F. Karsch et al, PLB 695, 136 (2011).
arXiv: 1203.0784; S. Borsanyi et al, JHEP1201,138(2011);

# Net-proton higher moments at 3 GeV from FXT (2018)

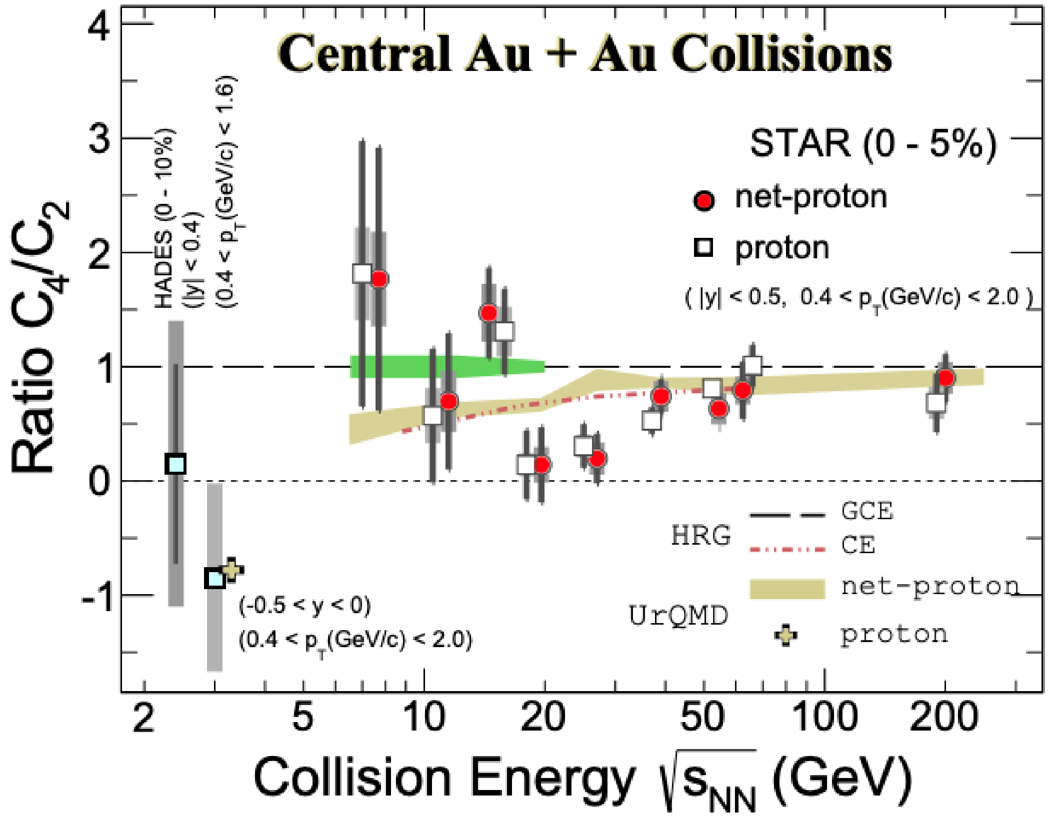


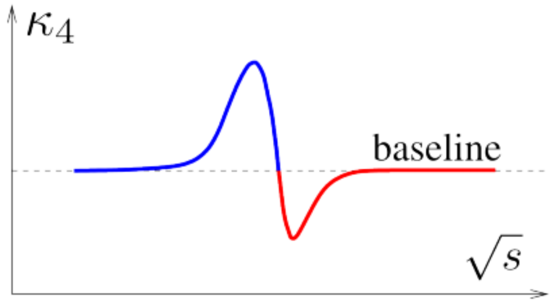


*BES-I: PRL 126 (2021) 092301*
*3 GeV data: PRL 128 (2022) 202303*

- Non-monotonic energy dependence in central Au+Au collisions (3.1$\sigma$)
- Strong suppression in proton $C_4/C_2$ at 3 GeV
  *- consistent with UrQMD hadronic transport model calculation*

# Disappearance of partonic collectivity in 3 GeV Au+Au collisions

Phys. Lett. B **827** (2022) 137003

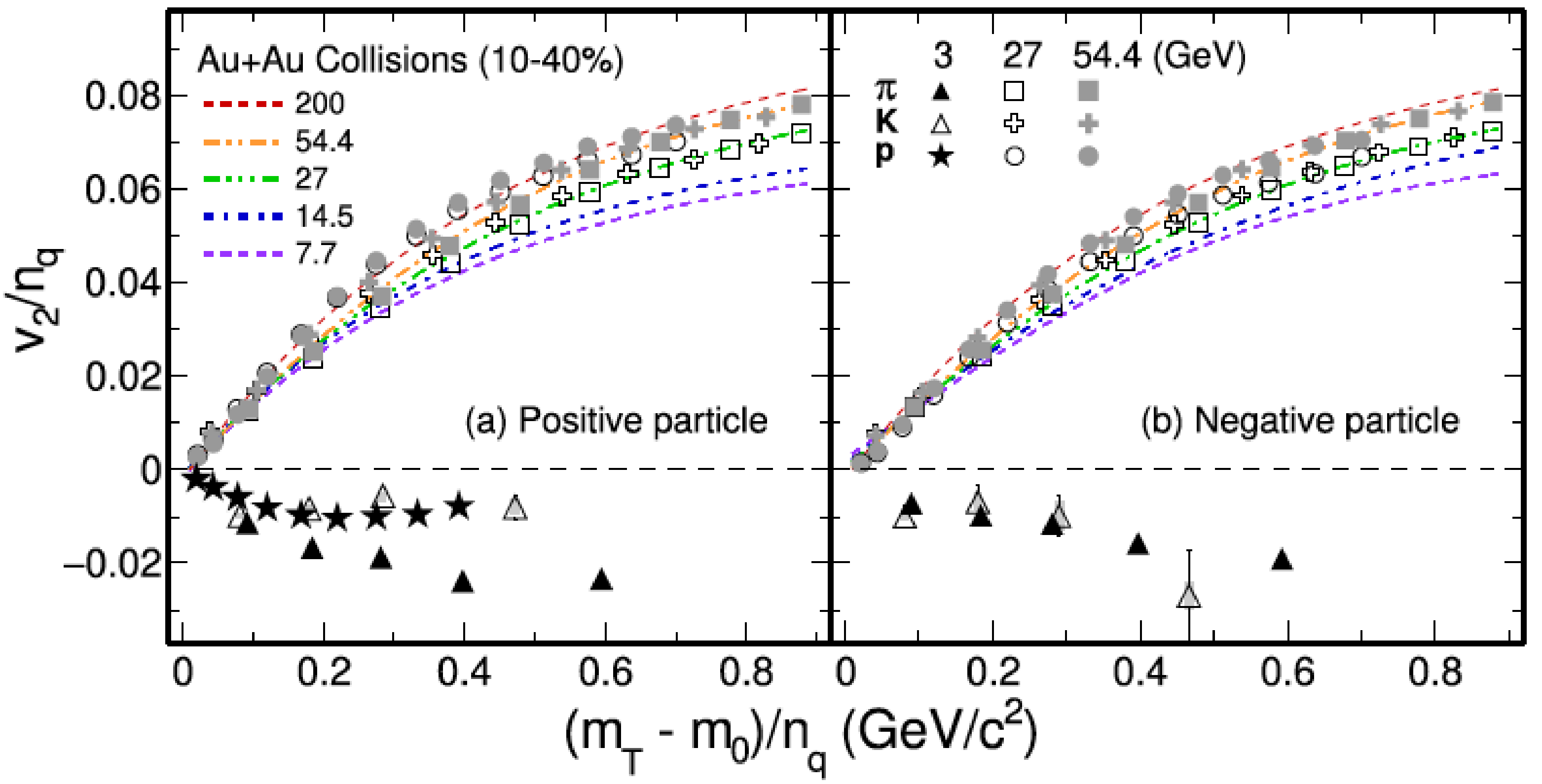


- Number of constituent quark (NCQ) scaling holds at 14.5 GeV and above
- No NCQ scaling and negative elliptic flow observed at 3 GeV

The results can be reproduced with a baryonic mean-field in transport model calculations.

Baryonic interactions dominate in 3 GeV Au+Au collisions

# Directed flow of hypernuclei

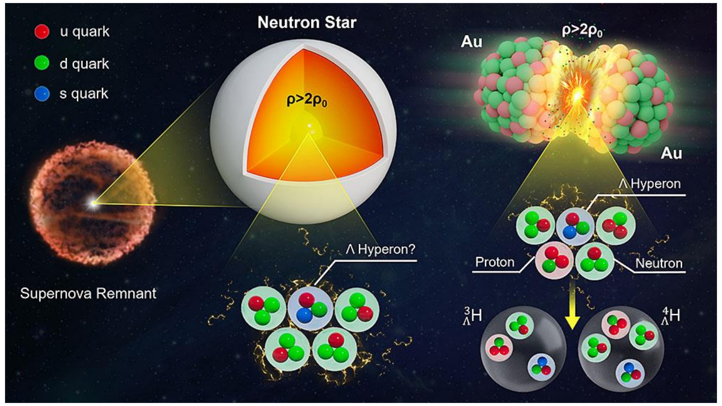


Picture credit:
BNL news article
https://www.bnl.gov/newsroom/news.php?a=121192

## Hypernuclei Production

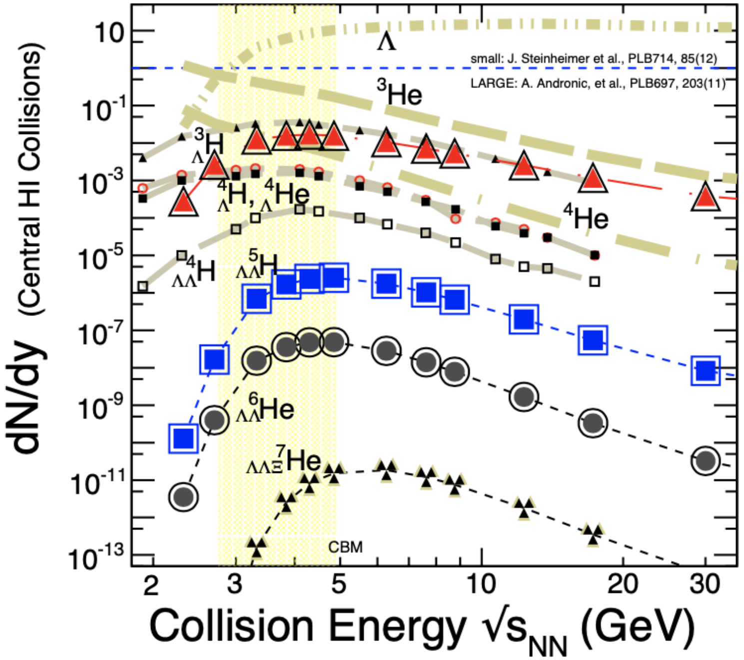


Constrain hyperon – nucleon and hyperon-hyperon interaction

Connection to neutron stars

PRL 130 (2023) 212301

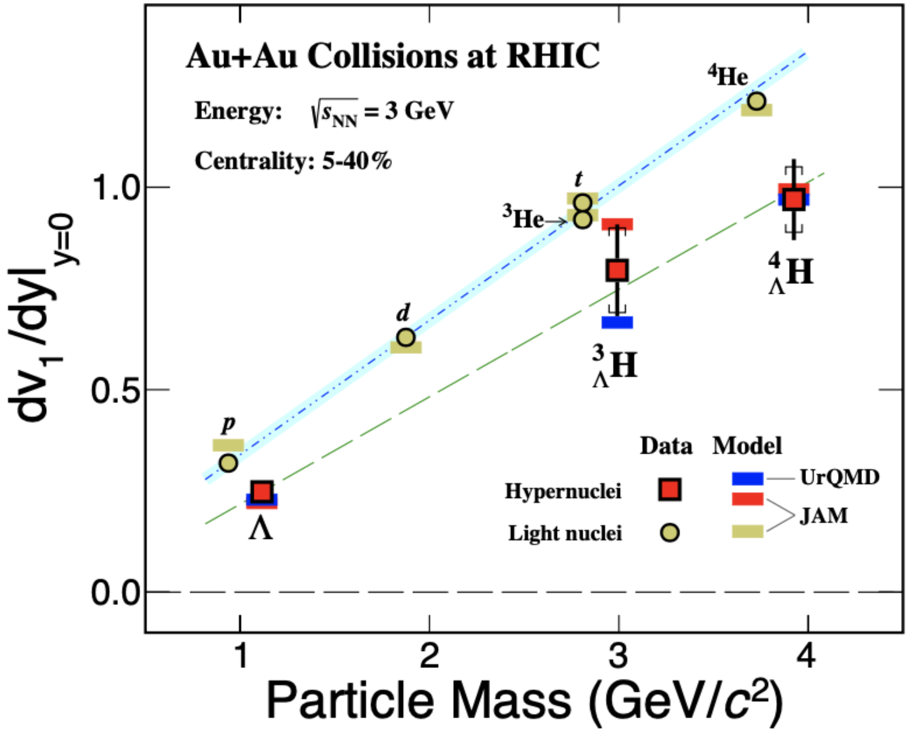


- First observation of significant hypernuclei directed flow in high energy nuclear collisions
- Midrapidity $v_1$ slopes follow baryon number scaling, implying that coalescence is the dominant production mechanism

Constrain hyperon-nucleon interactions at high baryon density

# STAR BES-II upgrades

Major improvements for BES-II

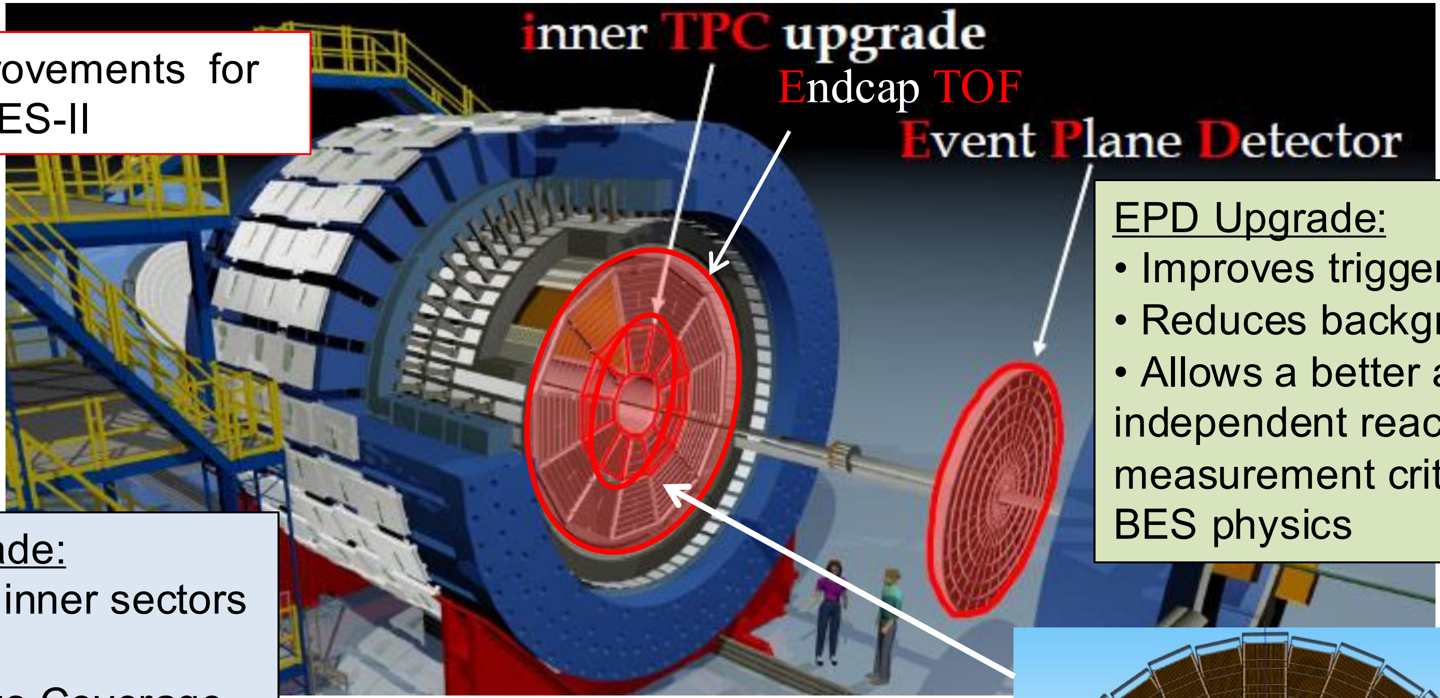


<u>EPD Upgrade:</u>
- Improves trigger
- Reduces background
- Allows a better and independent reaction plane measurement critical to BES physics

<u>iTPC Upgrade:</u>
- Replaced inner sectors of the TPC
- Continuous Coverage
- Improves dE/dx
- Extends η coverage from 1.0 to 1.5
- Lowers $p_T$ cut from 125 MeV/c to 60 MeV/c

<u>EndCap TOF Upgrade:</u>
- Rapidity coverage is critical
- PID at η = 1 to 1.5
- Improves the fixed target program
- Provided by CBM-FAIR

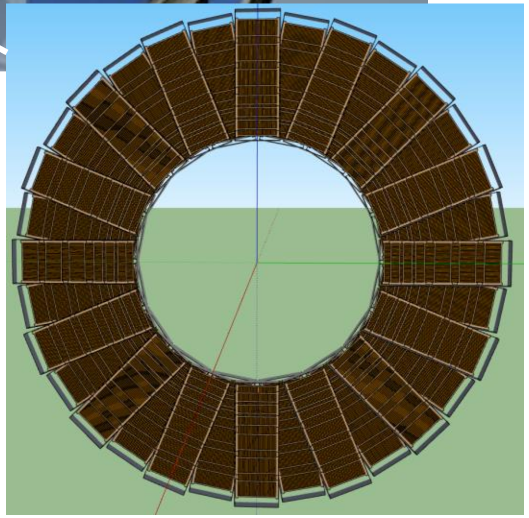

# Detector performance

## iTPC (2019+)

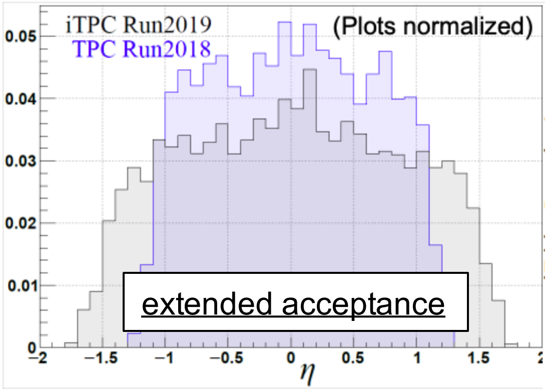


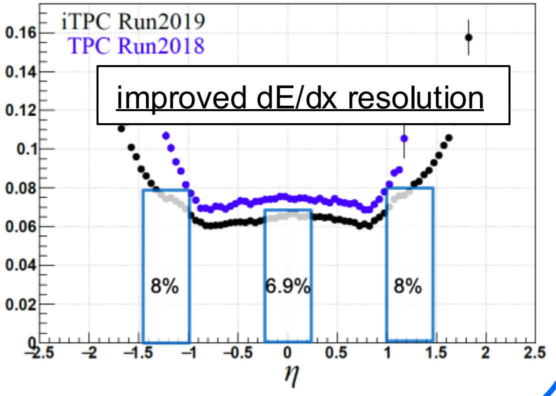


## eTOF (2019+)

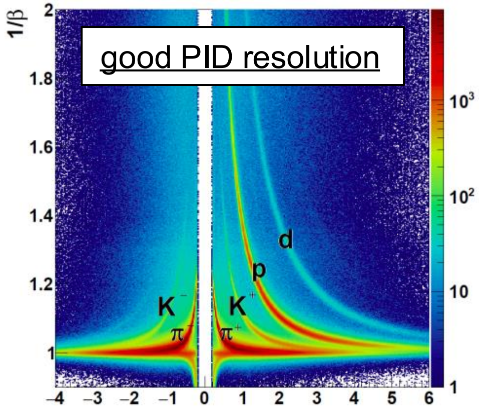


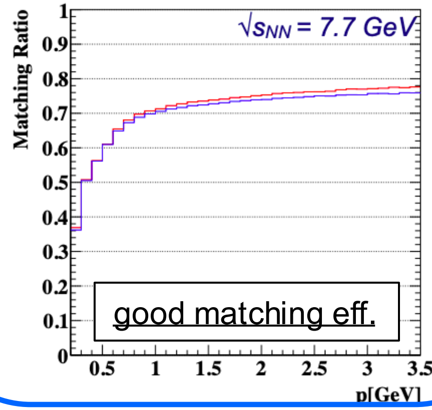


## EPD (2018+)

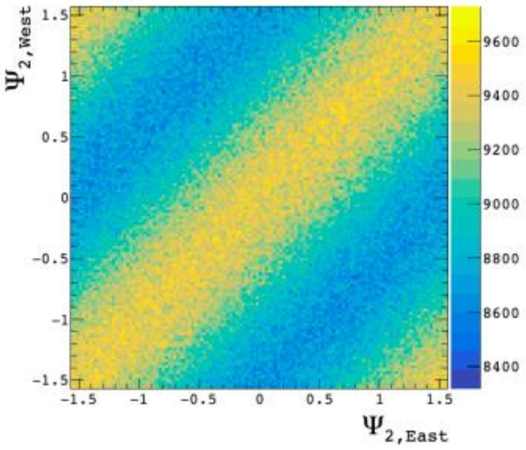


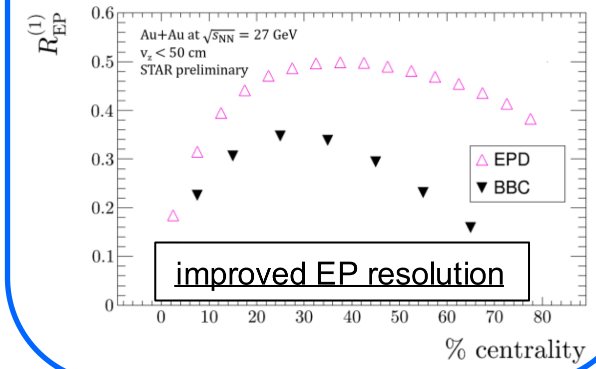

# BES-II datasets (2019-2021)

| Au+Au Collisions at RHIC | | | | | | | |
|---|---|---|---|---|---|---|---|
| Collider Runs | | | | Fixed-Target Runs | | | |
| | $\sqrt{s_{NN}}$ (GeV) | #Events | $\mu_B$ | | $\sqrt{s_{NN}}$ (GeV) | #Events | $\mu_B$ |
| 1 | 200 | 380 M | 25 MeV | 1 | 13.7 (100) | 50 M | 280 MeV |
| 2 | 62.4 | 46 M | 75 MeV | 2 | 11.5 (70) | 50 M | 316 MeV |
| 3 | 54.4 | 1200 M | 85 MeV | 3 | 9.2 (44.5) | 50 M | 372 MeV |
| 4 | 39 | 86 M | 112 MeV | 4 | 7.7 (31.2) | 260 M | 420 MeV |
| 5 | 27 | 585 M | 156 MeV | 5 | 7.2 (26.5) | 470 M | 440 MeV |
| 6 | 19.6 | 595 M | 206 MeV | 6 | 6.2 (19.5) | 120 M | 490 MeV |
| 7 | 17.3 | 256 M | 230 MeV | 7 | 5.2 (13.5) | 100 M | 540 MeV |
| 8 | 14.6 | 340 M | 262 MeV | 8 | 4.5 (9.8) | 110 M | 590 MeV |
| 9 | 11.5 | 257 M | 316 MeV | 9 | 3.9 (7.3) | 120 M | 633 MeV |
| 10 | 9.2 | 160 M | 372 MeV | 10 | 3.5 (5.75) | 120 M | 670 MeV |
| 11 | 7.7 | 104 M | 420 MeV | 11 | 3.2 (4.59) | 200 M | 699 MeV |
| | | | | 12 | 3.0 (3.85) | 260 + 2000 M | 750 MeV |

A broad $\mu_B$ coverage: $25 < \mu_B < 750$ MeV

BES-II data collected at RHIC cover a broad and interesting range of $\mu_B$ for the critical point search

# Net-proton higher moments from BES-II

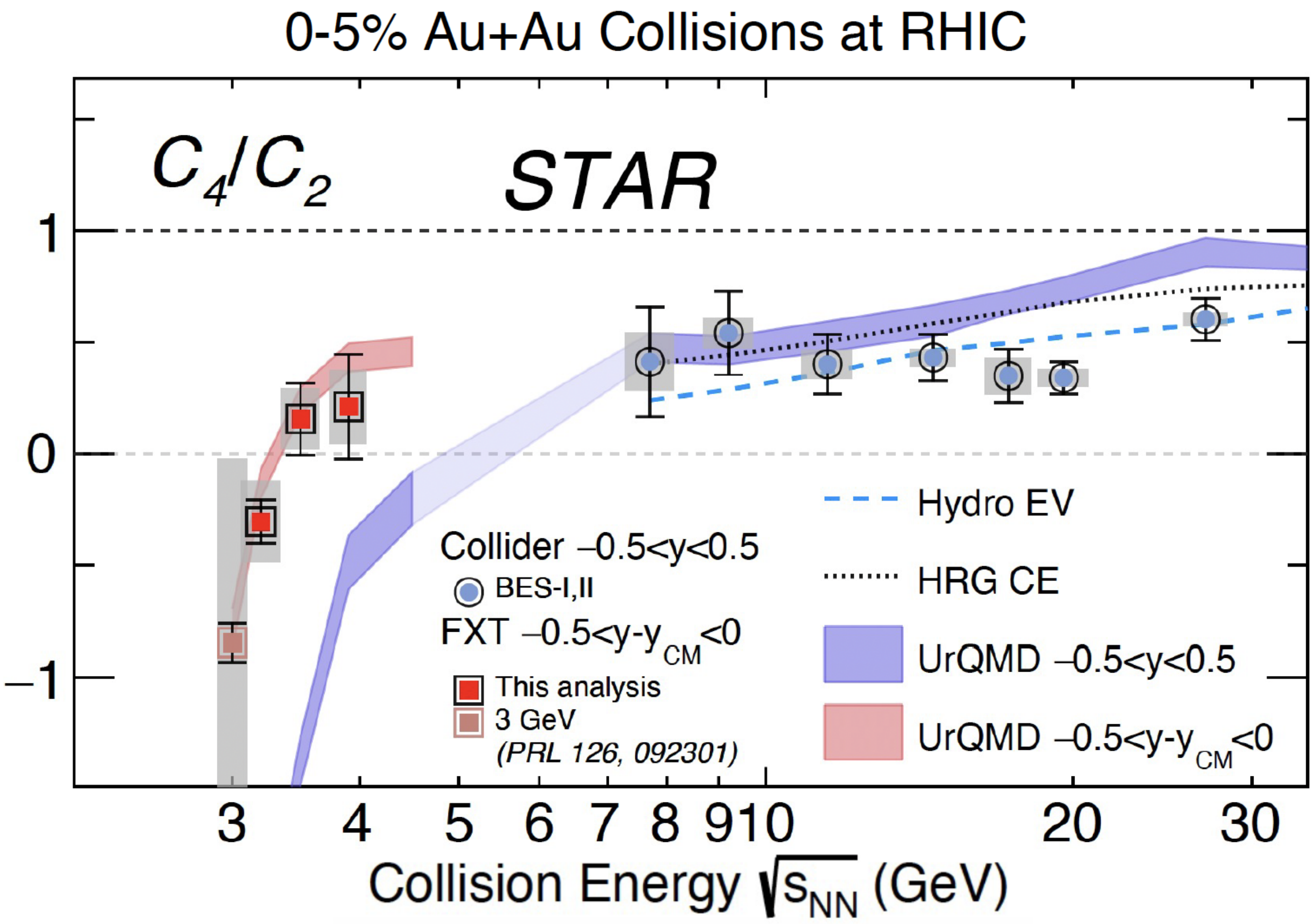

# Net-proton cumulants and proton factorial cumulants from 7.7 GeV to 27 GeV

**156 < $\mu_B$ < 420 MeV**

arXiv: 2504.00817

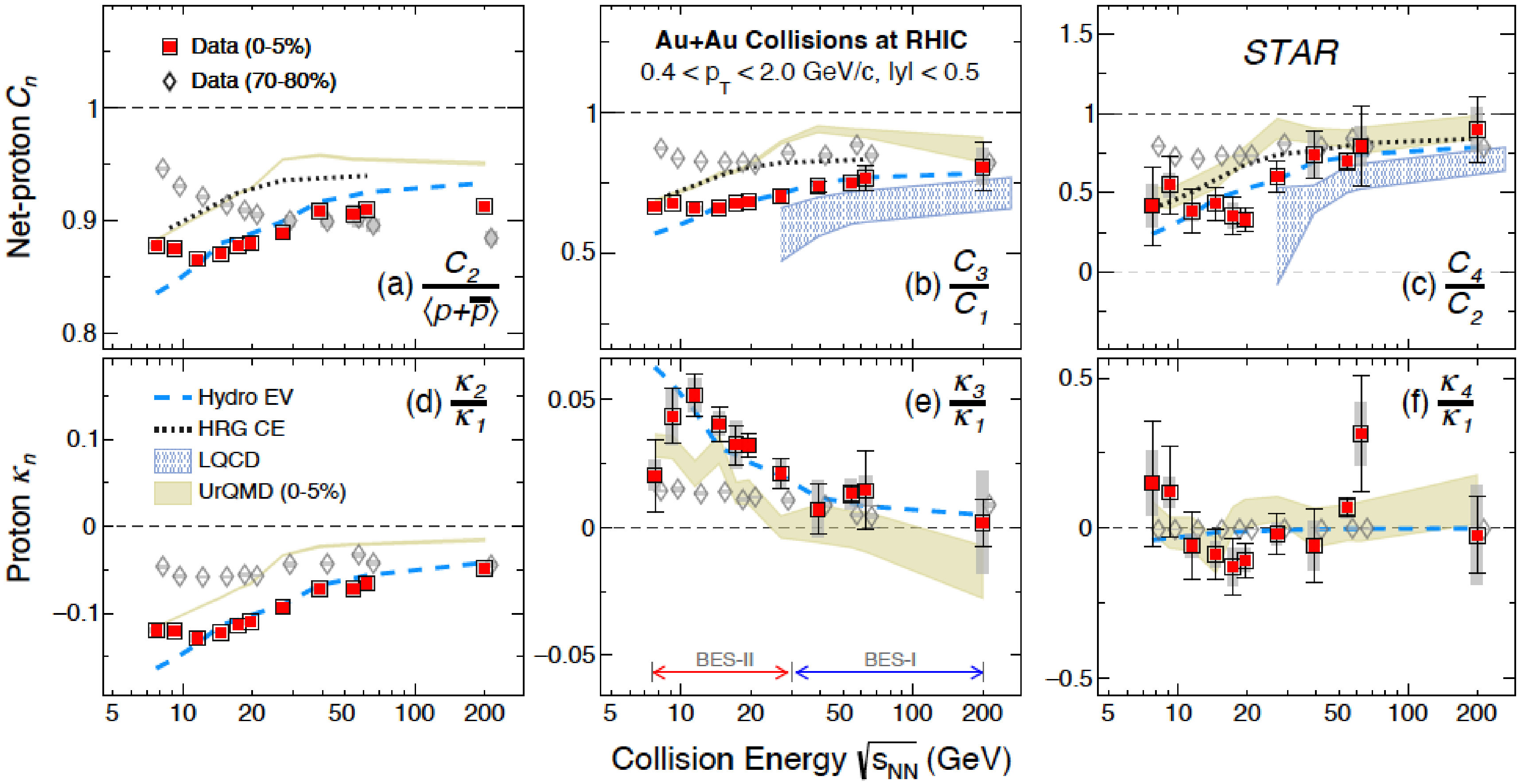


Precision results on net-proton cumulants and proton factorial cumulants from BES-II with greatly improved statistical and systematic uncertainties

**Reduction factor in uncertainties on 0-5% $C_4/C_2$ : BES-II vs BES-I**

| 7.7 GeV | | 19.6 GeV | |
|---|---|---|---|
| stat. error | sys. error | stat. error | sys. error |
| 4.7 | 3.2 | 4.5 | 4 |

Very interesting trends observed as a function of collision energy

Critical needs:

- Baseline calculations without critical point effects
- Dynamic calculations with critical point effects

# Net-proton cumulants and proton factorial cumulants from FXT energies

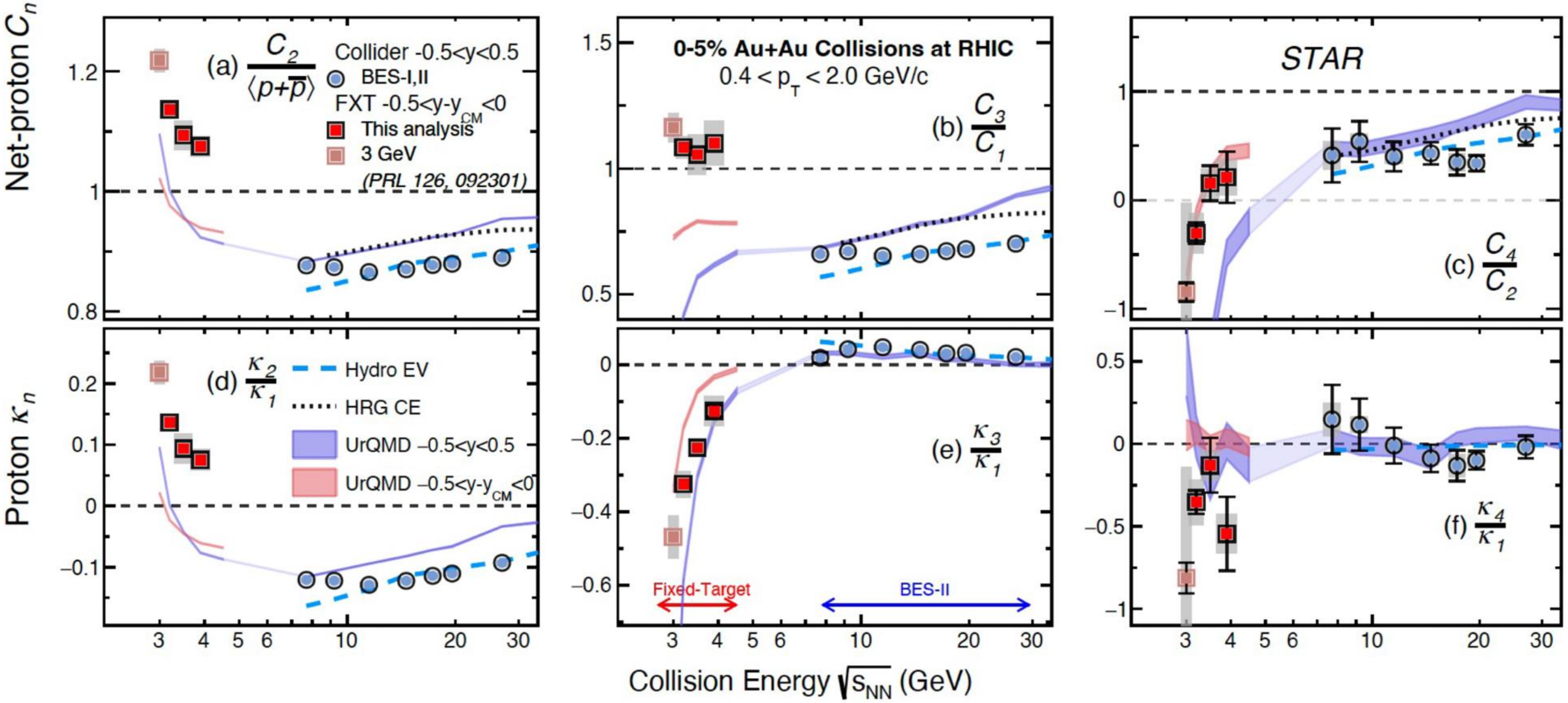


Proton $C_4/C_2$, $\kappa_4/\kappa_1$ consistent with UrQMD
Proton (factorial) cumulants deviate from UrQMD at second and third order

To do:

- Analyze 4.5 GeV and 2B 3 GeV data
- Study rapidity dependence

Critical needs:

- Baseline calculations without critical point effects
- Dynamic calculations with critical point effects

# Dynamical transverse momentum fluctuations

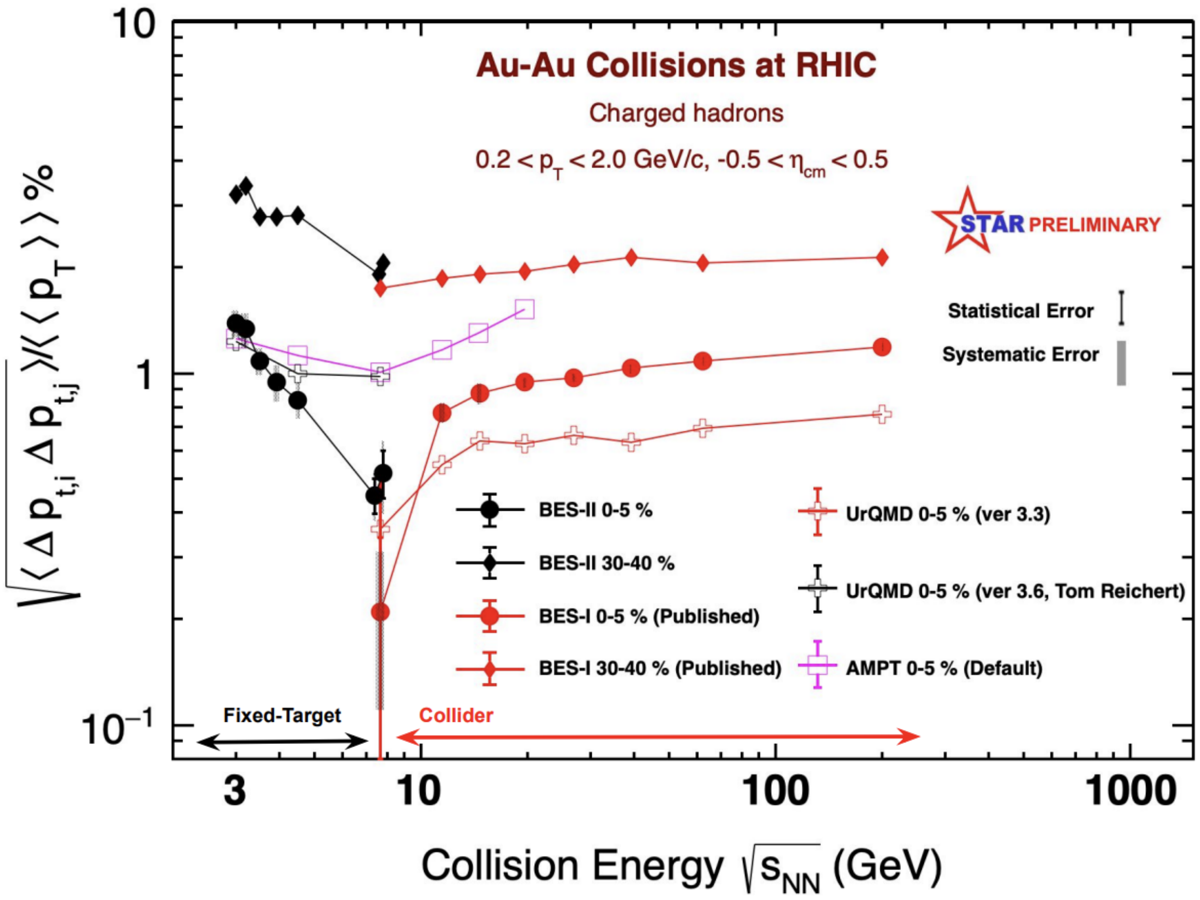


Non-monotonic energy dependence

To do:

- More comprehensive comparisons with baseline models

# NCQ scaling of elliptic flow

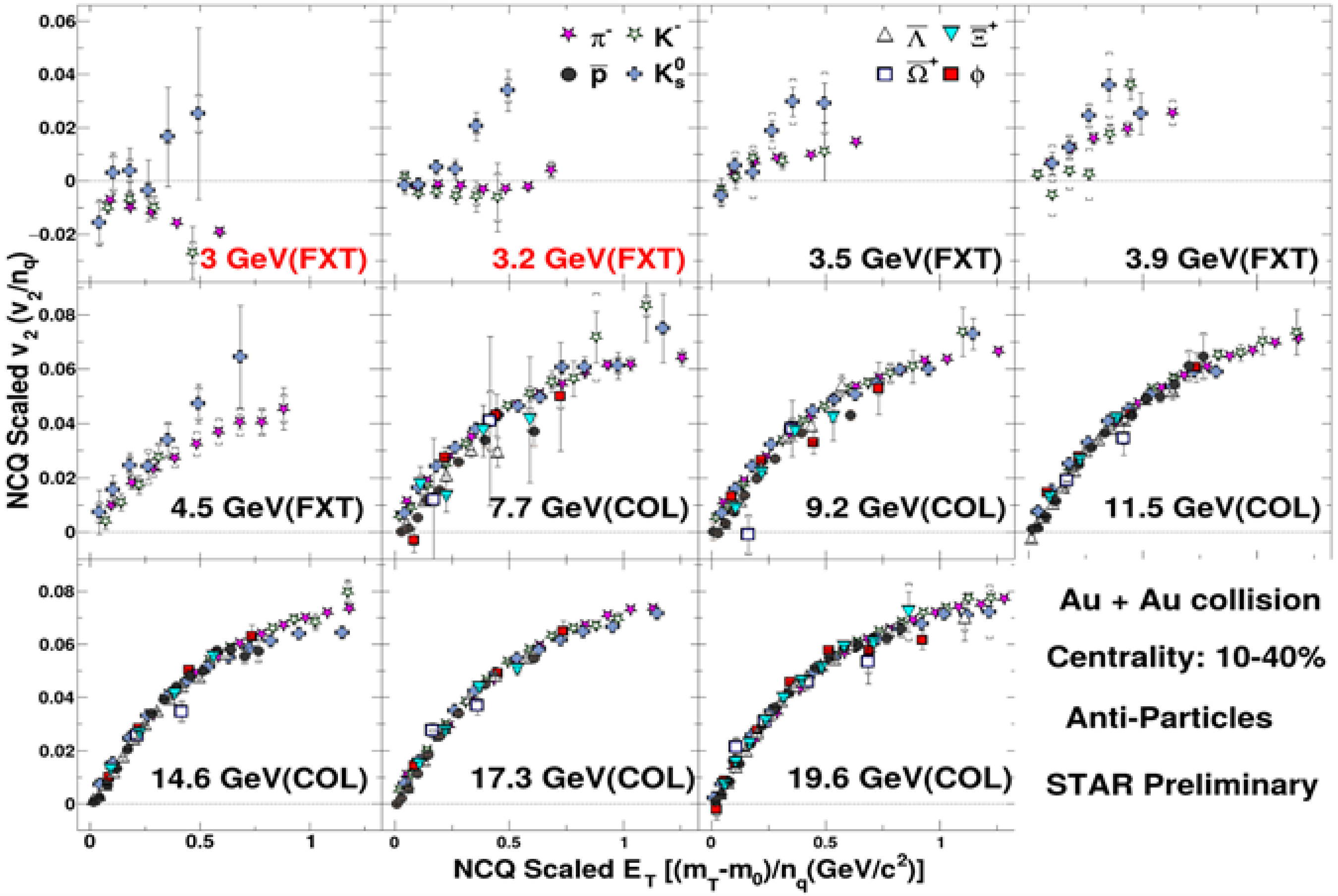


- NCQ scaling holds approximately for 7.7 GeV and above and completely breaks down at 3.2 GeV and below
  - Constraints on nuclear shadowing and the onset of partonic collectivity

# Directed flow of identified hadrons

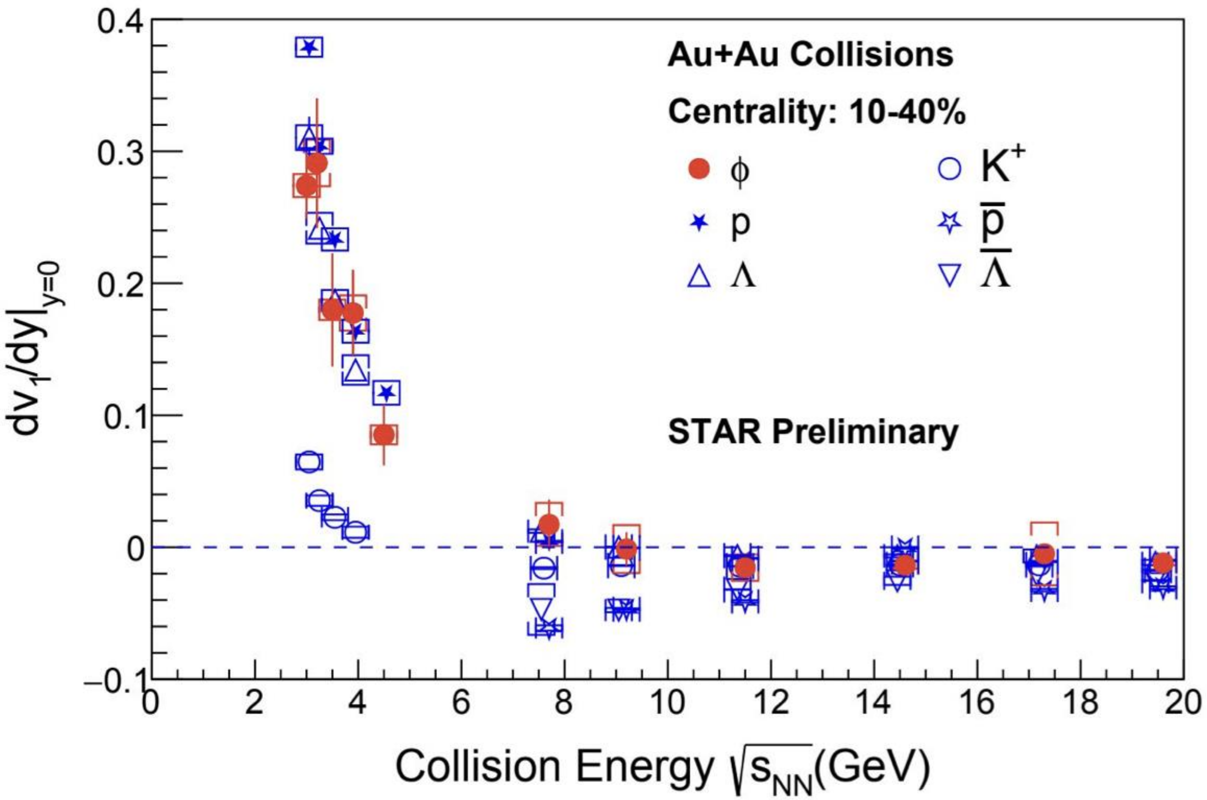


Sensitive to the very early stages of the collision

$v_1$ slope:

- φ meson behavior is similar to protons and lambdas
- Matches kaons at 9.2 GeV and above, but shows significant deviations in the FXT energy region

What is the underlying physics mechanism?

Momentum-dependent mean field potential at lower energies?

# Strange hadron production

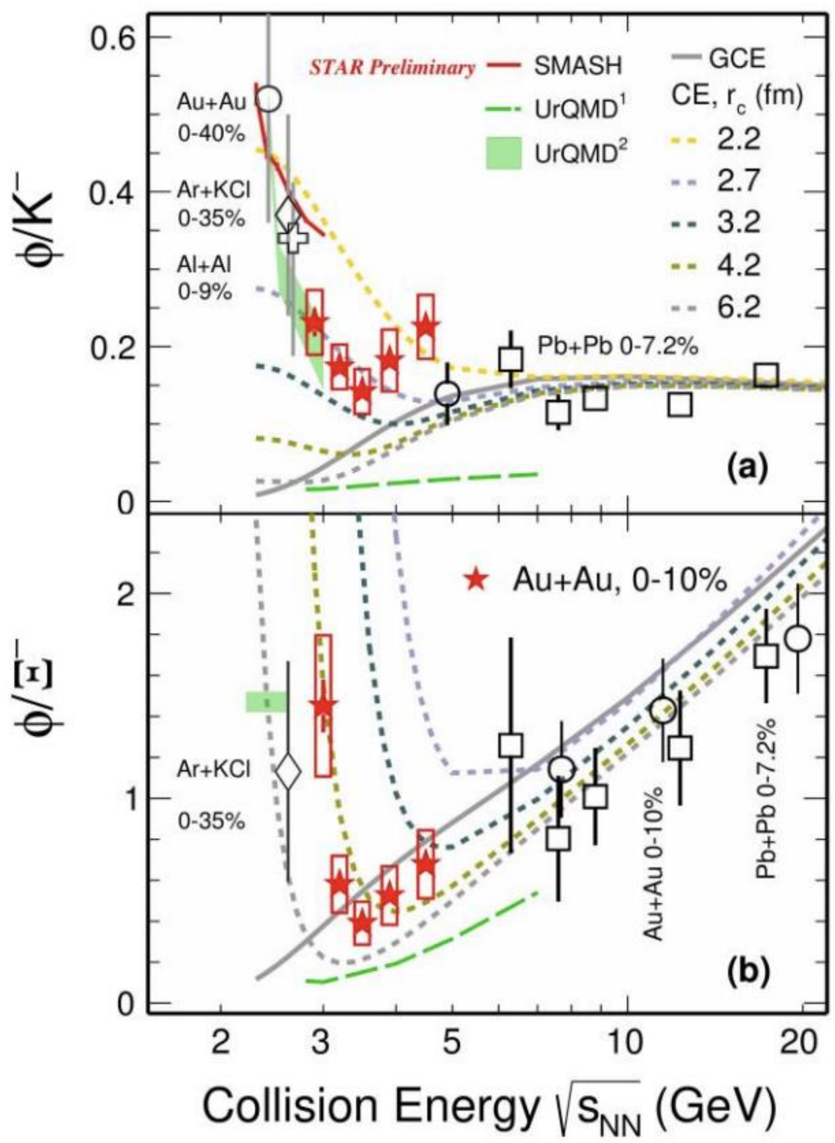


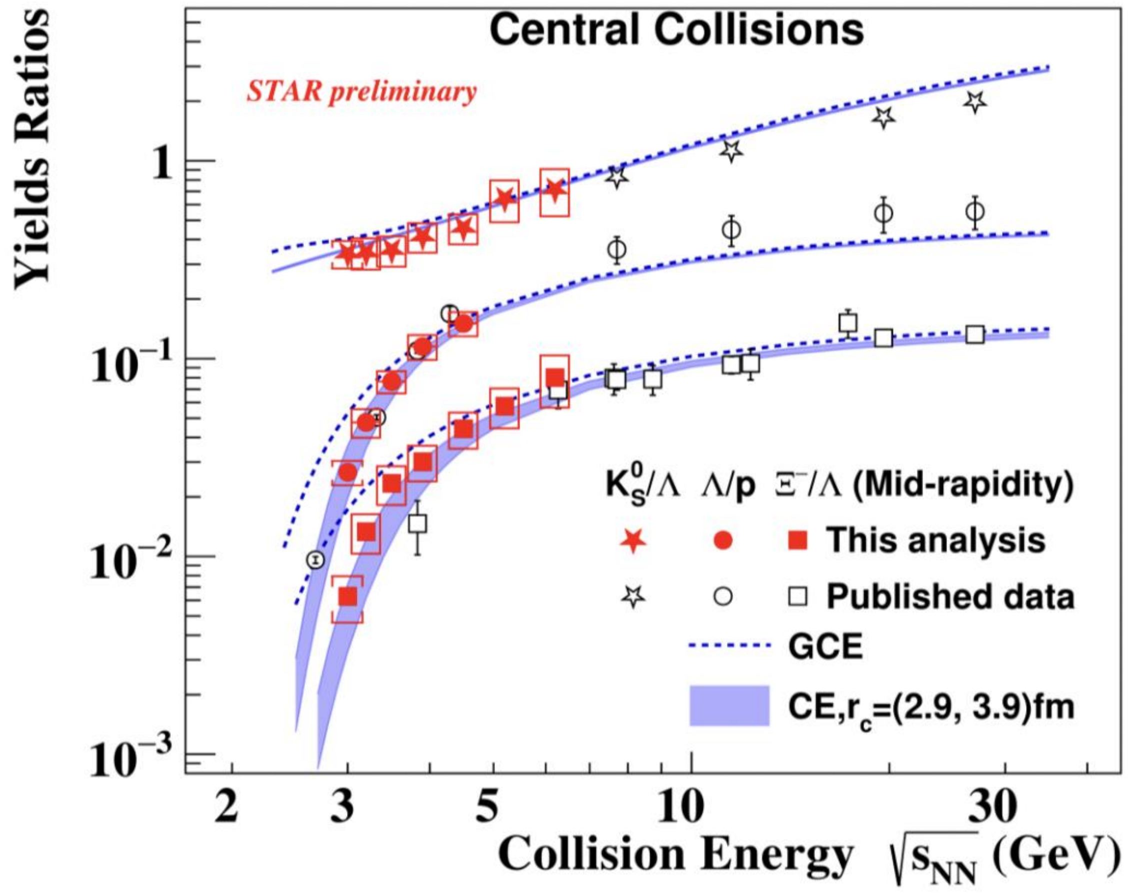


Strange hadron yield ratios deviate from Grand Canonical Ensemble expectations at collision energies below 5 GeV.

# Hypernuclei production

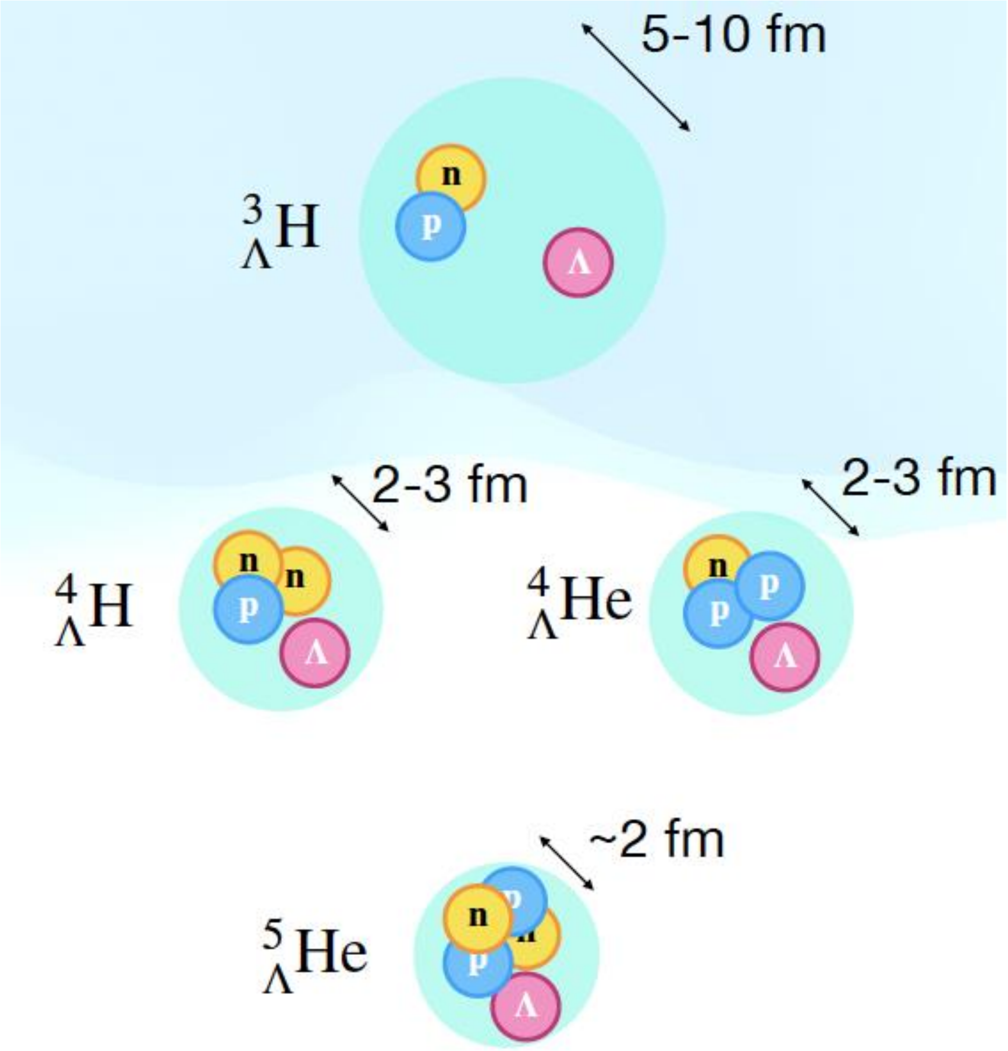


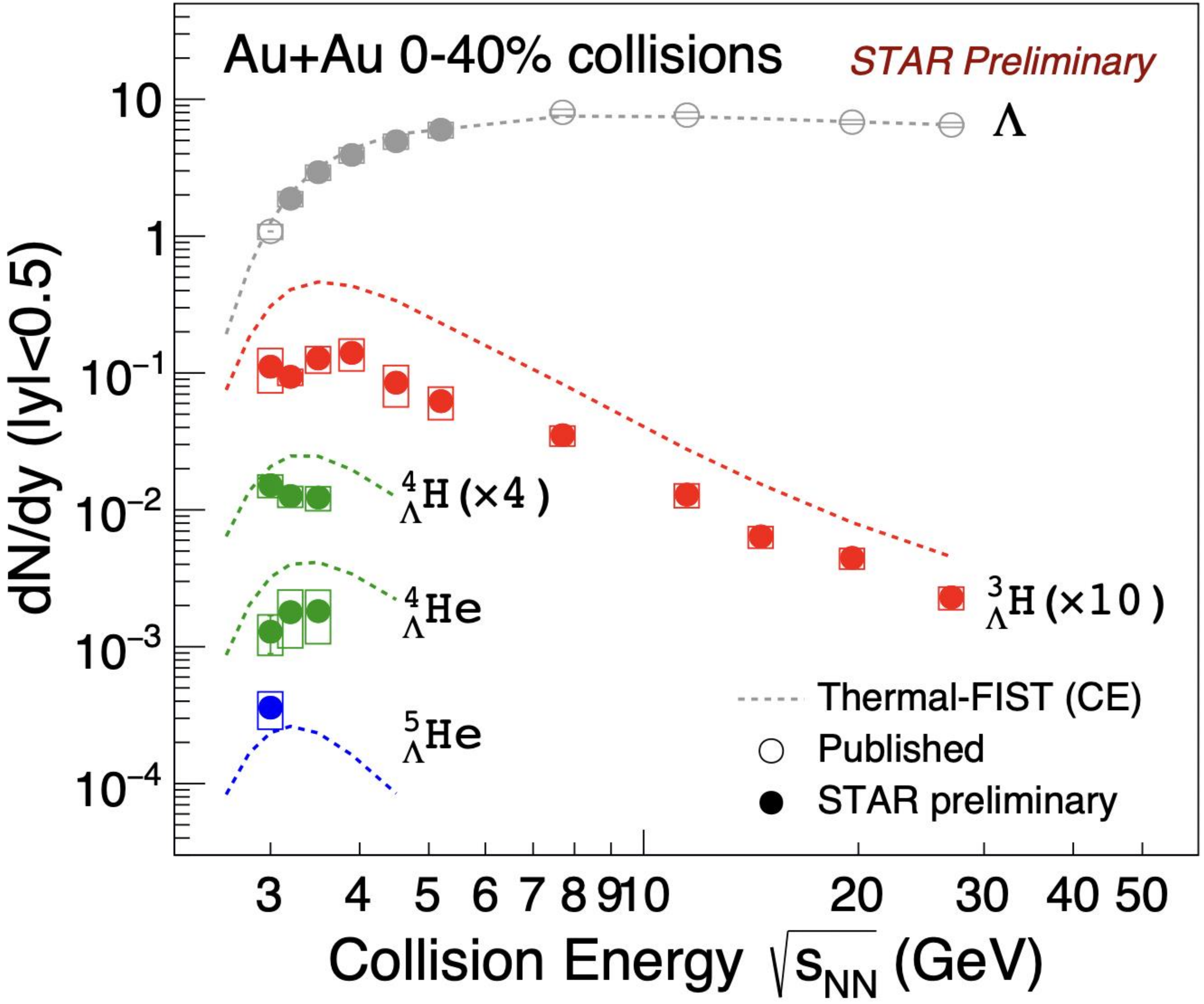

# Hypernuclei property

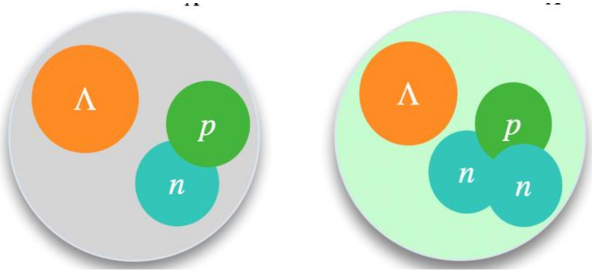


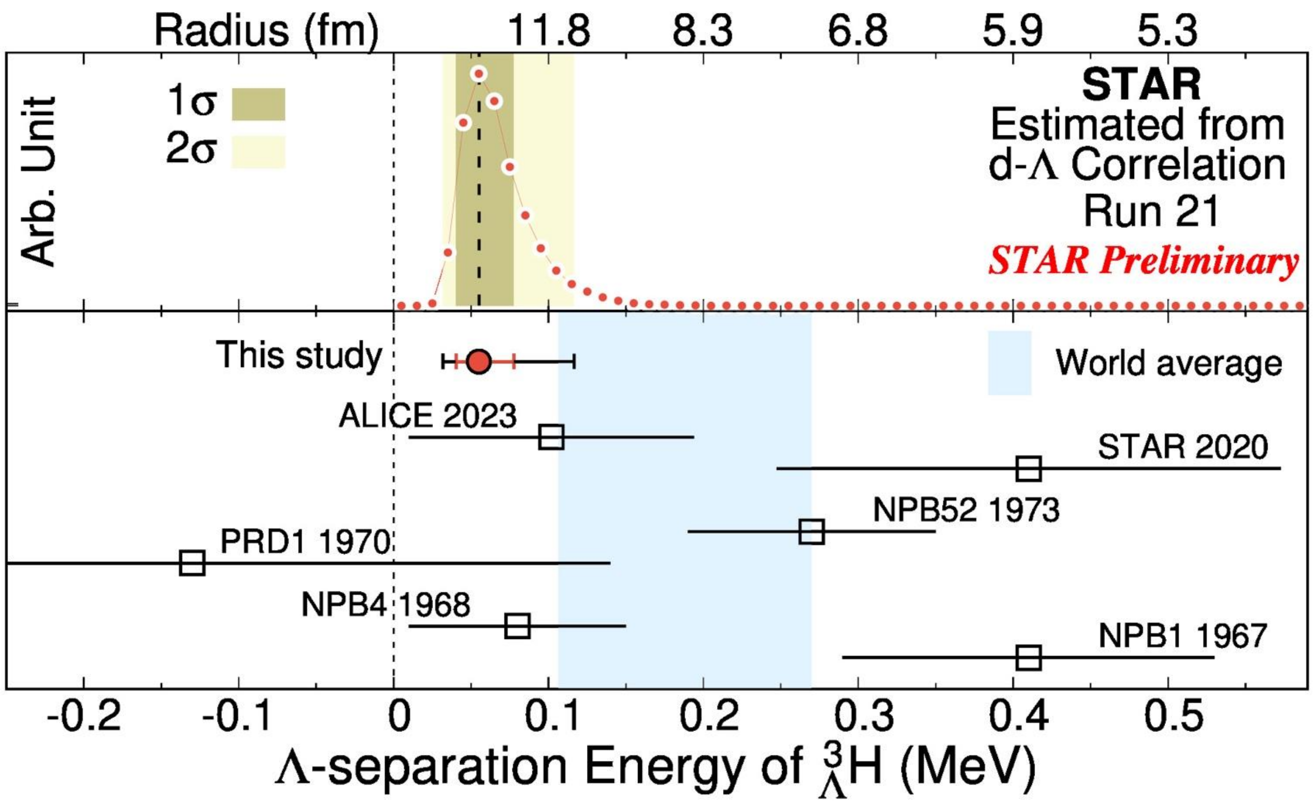


Most precise hypertriton lifetime measurement
via d-Lambda correlations

# Third body Coulomb interactions

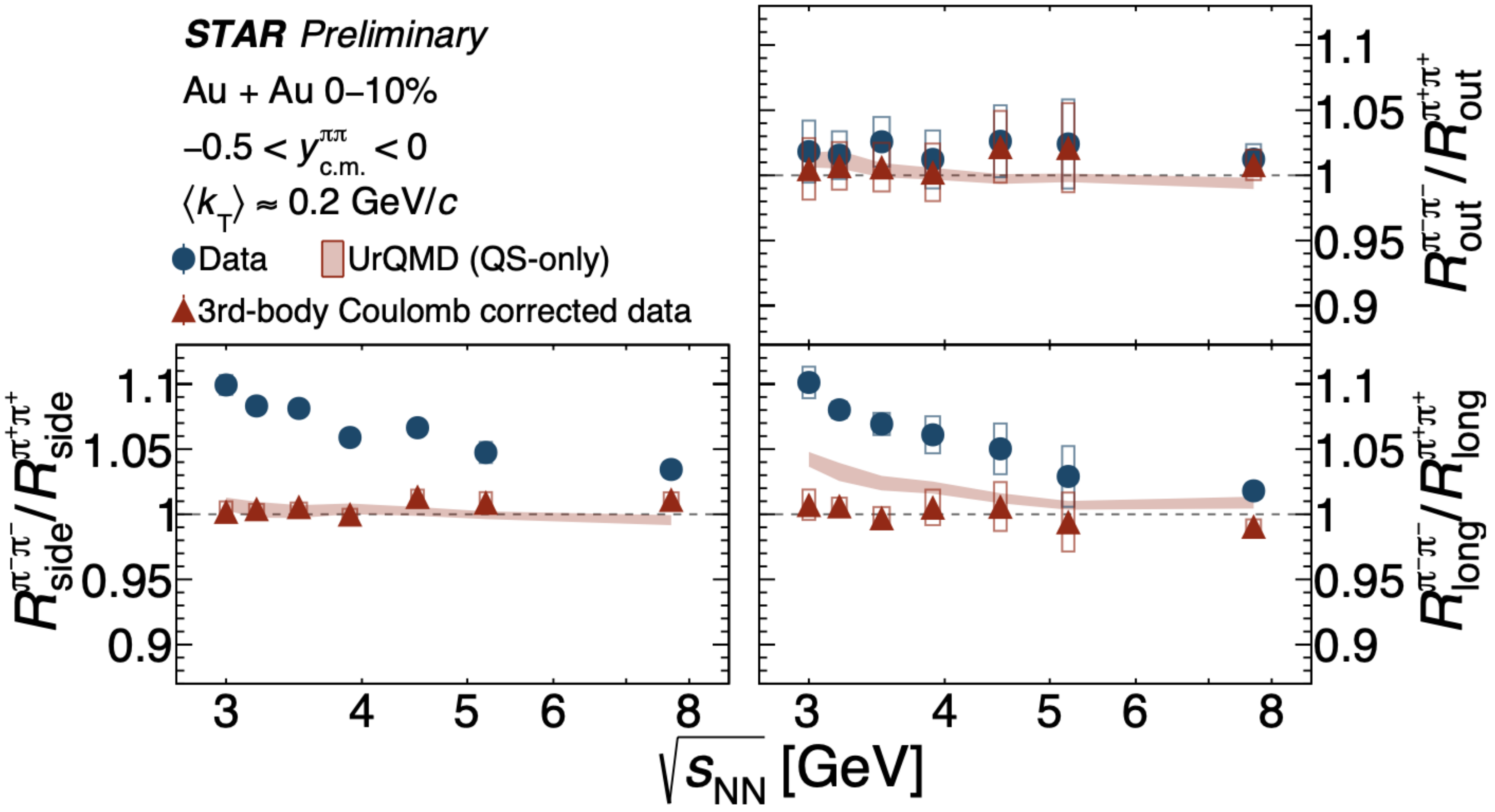


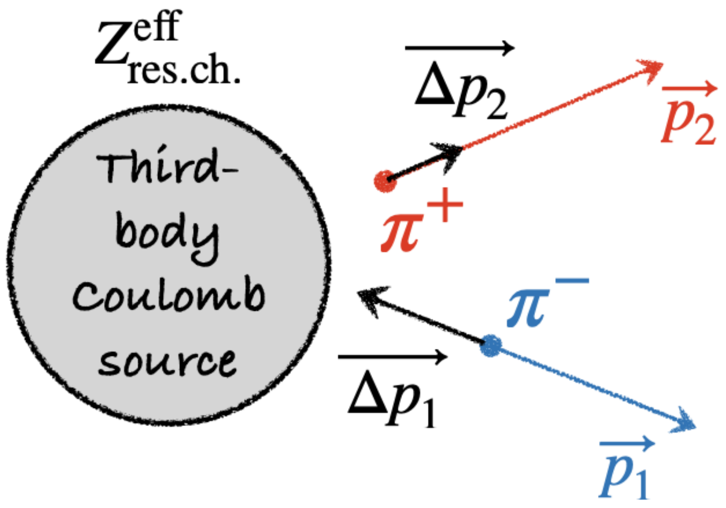


The measured femtoscopic source radii differ between $\pi^+\pi^+$ and $\pi^-\pi^-$ pairs

- Primarily due to the third-body Coulomb effect.
- No significant isospin effect.

# Conclusion

The STAR FXT program has been highly successful, thanks to many years of dedicated planning and preparation.

This program extends the baryon chemical potential ($\mu_B$) coverage up to 750 MeV, enabling us to:

- Search for the QCD critical point
- Explore signatures of a first-order phase transition
- Investigate the onset of QGP formation
- Study hyperon-nucleon interactions
- Examine the vorticity field in heavy-ion collisions
- Measure the freeze-out properties
- …

Stay tuned—many more exciting results are on the way!

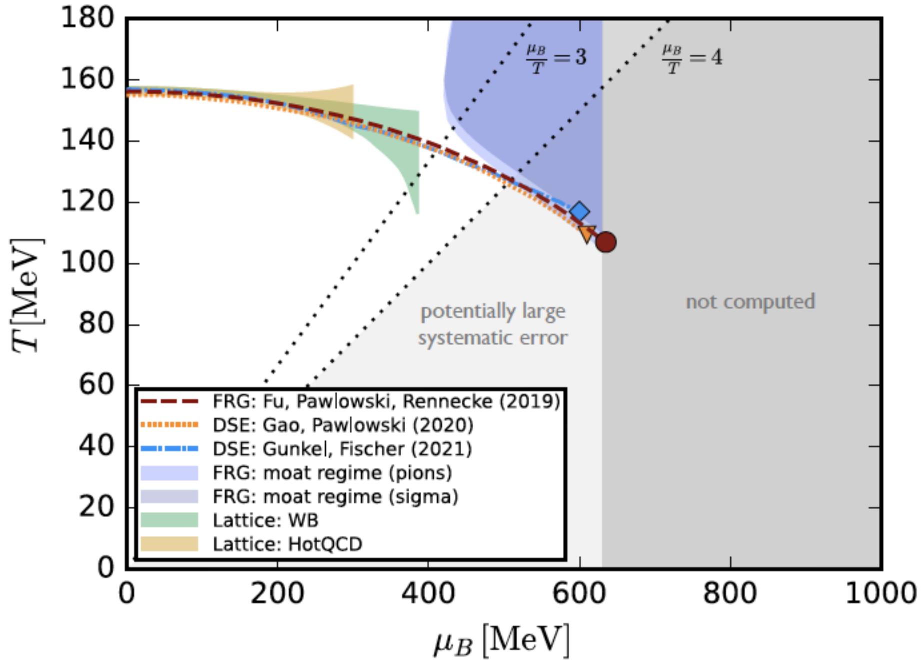


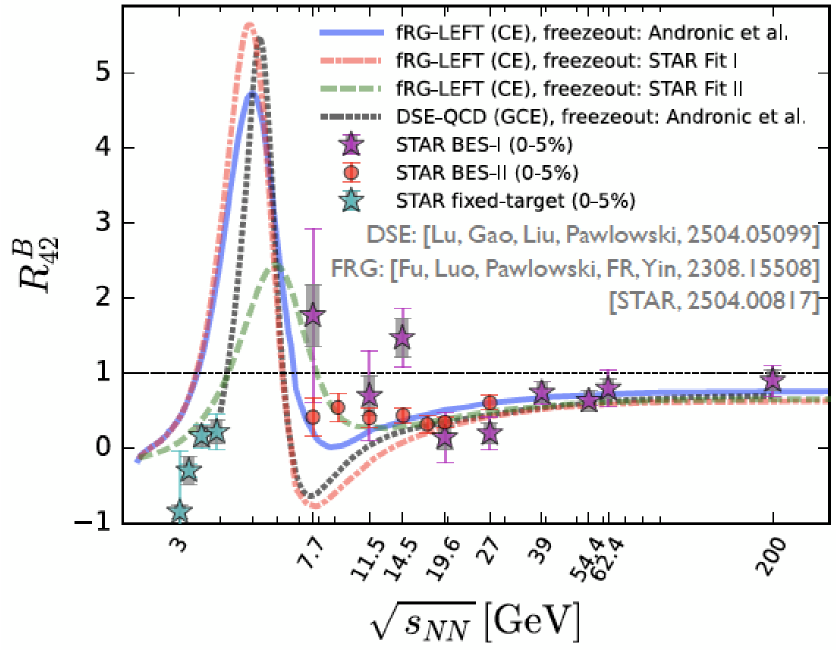


Fabian Rennecke, QM2025

# The future

## NA60$^{+}$ (2029)

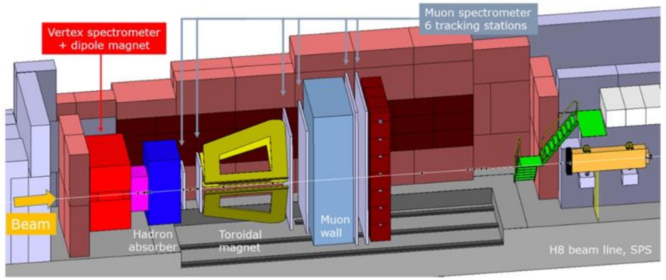


## NA61 (2008 - 2027)

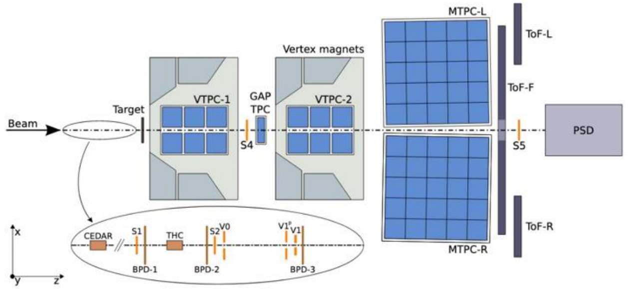


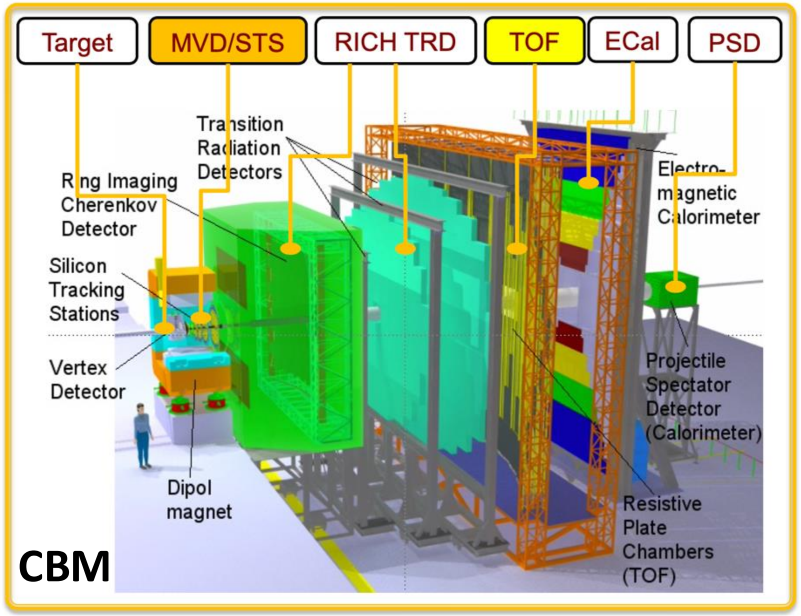


Physics opportunities in the exploration of the QCD phase diagram at high baryon density after the completion of the RHIC BES-II program: NA60+, NA61, CBM, NICA …

**Probe the physics of dense baryon-rich matter and constrain the nuclear equation of state in a regime relevant to binary neutron star mergers and supernovae.**